Bubble shapes in steady axisymmetric flows at intermediate Reynolds number

G. Ryskin and L. G. Leal

Department of Chemical Engineering, California Institute of Technology, Pasadena, CA 91125

Abstract

We consider the shape of a gas bubble which rises through a quiescent incompressible, Newtonian fluid at intermediate Reynolds numbers. Exact numerical solutions for the velocity and pressure fields, as well as the bubble shape, are obtained using finite difference techniques and a numerically generated transformation to an orthogonal, boundary-fitted coordinate system. No restriction is placed on the allowable magnitude of deformation.

Introduction

In spite of intensive investigation for more than 70 years, the theoretical problem of bubble and drop motion in an unbounded viscous Newtonian liquid, which may either be quiescent or undergoing some prescribed motion far from the bubble or drop, has remained essentially unsolved. The main difficulty, in addition to the usual nonlinearity of the equations of motion at finite Reynolds number, is that the bubble or drop shape is unknown and required as part of the solution of the problem. As a consequence, the boundary conditions at the bubble or drop surface are nonlinear, and, in addition, the solution depends on the prior history of the bubble or drop motion and interface shapes, even in the creeping motion limit.

This problem of bubble or drop motion in a viscous liquid, with an unknown boundary shape, is an example of the general class of so-called "free boundary" problems of fluid mechanics. Although a number of methods exist for this type of problem, which can be used to analyze the motion of bubbles or drops, all but purely numerical methods inevitably suffer from some restriction. Included is the asymptotic technique of "domain perturbations" which has been applied, for example, for buoyancy-driven motions of a drop at finite Reynolds,[1] and for a drop in a general linear "shear" flow,[2] but is restricted to small deformations from a known (or guessed) boundary shape. Boundary integral techniques are not restricted in the degree of deformation (and thus provide a powerful tool to study bubble and drop deformation[3-5]), but are only applicable in the limits of either creeping flow, or potential flow, where the governing differential equations are linear. For more general conditions, this leaves us with numerical methods which are not limited, in principle, either by the allowable degree of deformation or by linearity of the governing equations. Such methods have not been applied directly to the problem of calculating bubble or drop shapes in viscous flow so far as we are aware. However, in most other applications to free boundary problems in fluid mechanics, the numerical methods of choice have been based upon finite element formulations. At least in part, this has been a consequence of the loss of accuracy which occurs when finite difference techniques are applied in domains with boundaries that are not coincident with coordinate lines or surfaces. Thus, if one considers only the classical orthogonal coordinates, such as cylindrical, spherical, etc., the use of finite-difference methods is generally unacceptable for free boundary problems. The present paper explores the alternative possibility of finite-difference solutions based on a numerical method of constructing a system of orthogonal, boundary-fitted coordinates, for the problem of streaming flow past a bubble. We do not claim or intend to imply "superiority" in any sense over other possible numerical approaches to the same problem. Indeed, the methods described here are not at a sufficiently advanced stage of development for such comparisons to be meaningful, even if one were philosophically inclined to make them!

A detailed description of the methods of orthogonal mapping will soon appear in the *Journal of Computational Physics*,[6] and a more detailed description of methods and results for the application to the motion of a bubble or drop in a viscous fluid is presently in preparation. Here, we simply outline the method of solution and present two examples of the solution for streaming flow past a bubble at finite Reynolds number as an illustration of its application.

Orthogonal Mapping

The idea which we pursue is thus to obtain orthogonal boundary-fitted coordinates for the domain exterior to a bubble whose shape is unknown, though smooth and generally nonspherical. In the present development, the unknown shape is generated via an iterative procedure starting from some initial guess. At each step, with the boundary shape specified, mapping functions for the boundary-fitted coordinates are generated numerically, the equations of motion are then solved in the transform domain and the normal stress balance at the bubble surface is used to generate an improved shape. We restrict ourselves to steady, axisymmetric configurations and discuss the mapping problem in 2D, with the axisymmetric boundary shape generated by rotation about the axis of symmetry which is thus required to be a coordinate line for the transform coordinates.

In the remainder of this section, we outline a method of obtaining the desired coordinate transformation. From a mathematical point of view, we require a pair of functions $x(\xi,\eta)$ and $y(\xi,\eta)$ which map points of the physical domain onto a unit square, $0 \le \xi,\eta \le 1$, in the transform domain, with lines of constant ξ and η being orthogonal. For convenience, we designate the bubble surface as $\xi = 1$, and the upstream and downstream

axes of symmetry as $\eta = 1$ and $\eta = 0$, respectively, with $\xi \to 0$ corresponding to infinity. There has, of course, been a great deal of recent research aimed at the problem of obtaining numerically generated coordinate mappings. Included in this work are methods based on the solution of a pair of elliptic equations for the mapping functions,[7] conformal mapping,[8] direct integration of "Cauchy-Riemann"-type equations as an initial value problem starting from a boundary[9,10] and other methods of orthogonal mapping which are equivalent to conformal mapping with less restrictive constraints on the ratio of the diagonal components of the metric tensor (the latter are, in fact, most closely related to the present approach).[11-13] Limitations of space prevent a detailed review of this prior work. However, in general, the resulting coordinate systems are either nonorthogonal,[7] ill-conditioned in the sense of extreme sensitivity to boundary shape and/or (the possibility of) highly nonuniform spacing of coordinate lines (conformal mapping,[8] some types of "orthogonal mapping"[11,12]) or only suitable in some local subdomain (integrations of Cauchy-Riemann equations[9,10]).

The present objective is a numerically generated mapping which is applicable in the whole domain, automatically orthogonal and free of the usual sensitivity problems of conformal mapping. Our basis is conventional tensor analysis, yielding equations for $x(\xi,\eta)$ and $y(\xi,\eta)$ which are coordinate invariant. These equations follow almost trivally from the observation that a Cartesian coordinate x (or y) is a linear scalar function of position, so that grad x (or grad y) is constant and

$$\text{div grad } x = 0 \tag{1}$$

The latter is nothing more than the covariant Laplace equation for x. When expressed in terms of the desired (but as yet unspecified) ξ,η coordinates, it becomes

$$g^{ij}x_{;ij} = 0 \tag{2}$$

in which g^{ij} is the ij component of the metric tensor and ";" denotes regular covariant differentiation. Although the solutions of Eq. (1) (and the similar equation for y) will not generally yield orthogonal coordinates, we further specify that

$$g_{ij} = 0 \qquad \text{for} \qquad i \neq j \tag{3}$$

and

$$g_{11} = h_\xi^2 , \quad g_{22} = h_\eta^2 \tag{4}$$

with the $h_\xi . h_\eta$ being "scale" factors for the ξ,η system. In this case, the equations governing the transformation (mapping) functions become

$$\frac{\partial}{\partial \xi}\left(f \frac{\partial x}{\partial \xi}\right) + \frac{\partial}{\partial \eta}\left(\frac{1}{f}\frac{\partial x}{\partial \eta}\right) = 0 \tag{5a}$$

$$\frac{\partial}{\partial \xi}\left(f \frac{\partial y}{\partial \xi}\right) + \frac{\partial}{\partial \eta}\left(\frac{1}{f}\frac{\partial y}{\partial \eta}\right) = 0 \tag{5b}$$

with

$$f(\xi,\eta) \equiv h_\eta / h_\xi \tag{6}$$

and the solution of these equations, subject to appropriate boundary conditions (which we shall discuss in the next section), will yield orthogonal coordinates for any f, which can thus be chosen freely. It may be noted that conformal mapping corresponds to the restrictive choice $f(\xi,\eta) = 1$, for all ξ,η.

In general, the "most appropriate" choice of f depends on the type of mapping required. The problem of direct mapping with fixed boundary shape and a specified distribution of coordinate nodes along the boundary is discussed elsewhere.[6] Here, we consider only the mapping problem in which the boundary shape is unknown and required as part of the solution of the overall problem. In this case, $f(\xi,\eta)$ can be specified directly as a function of ξ,η, with the form for f chosen so as to yield desired properties of the transform coordinates (e.g. nonuniform spacing of coordinate lines in some region of the domain).

The fluid dynamics problem – basic formulation

Let us now return to the problem of uniform streaming flow past a bubble. In this case, we adopt the very simple form for f, $f(\xi,\eta) = \pi\xi$. In addition, we introduce a relatively simple modification of the mapping procedure outlined above to take care of the fact that infinite values of the mapping functions x and y, corresponding directly to an infinite domain, cannot be generated numerically. To avoid this difficulty, we simply calculate the mapping from the unit square in the ξ,η plane to an auxiliary finite domain, which is then transformed to the physical domain by a conformal inversion.

Now, one great advantage of orthogonal coordinates, in addition to avoiding inaccuracy of numerical approximation in nonorthogonal coordinates, is that physical components of vectors and tensors can be used instead of covariant or contravariant ones. The governing Navier-Stokes equations, plus boundary conditions, can thus be expressed in a straightforward manner in terms of the resulting boundary-fitted coordinates

ξ,η,ϕ, obtained by rotation of the two-dimensional coordinates given by $x(\xi,\eta)$ and $\sigma(\xi,\eta)$ (where x is parallel to the axis of symmetry and σ is the distance to this axis along a normal through the point of interest). If we introduce the streamfunction ψ, and use standard expressions for the invariant differential operators in general orthogonal curvilinear coordinates, the Navier-Stokes equations are

$$\frac{1}{h_\xi h_\eta}\frac{\partial\psi}{\partial\eta}\frac{\partial}{\partial\xi}\left(\frac{\zeta}{\sigma}\right) - \frac{1}{h_\xi h_\eta}\frac{\partial\psi}{\partial\xi}\frac{\partial}{\partial\eta}\left(\frac{\zeta}{\sigma}\right) = \frac{2}{Re}L^2(\zeta\sigma) \tag{7}$$

$$L^2\psi + \zeta = 0 \tag{8}$$

where ζ is the vorticity, $Re = \frac{d\rho v_\infty}{\mu}$, d is the equivalent diameter of the bubble and

$$L^2 \equiv \frac{1}{h_\xi h_\eta}\left\{\frac{\partial}{\partial\xi}\left(\frac{f}{\sigma}\frac{\partial}{\partial\xi}\right) + \frac{\partial}{\partial\eta}\left(\frac{1}{f\sigma}\frac{\partial}{\partial\eta}\right)\right\} \tag{9}$$

The streamfunction at infinity, for a uniform streaming flow, takes the form

$$\psi_\infty = \frac{1}{2}\sigma^2 \tag{10}$$

Thus, to avoid dealing with large (or infinite) numbers, we actually solve for

$$\psi^* = \psi - \psi_a \tag{11}$$

where ψ_a is the potential flow solution for flow past a spherical bubble with the given form ψ_∞ at infinity, i.e.

$$\psi_a = \frac{1}{2}\sigma^2(1 - \xi^3) \tag{12}$$

Now, Eqs. (4) and (5), rewritten in terms of ψ^*, are to be solved for ψ^*, ζ and the bubble shape subject to the boundary conditions

$$\psi^* \text{ is bounded, } \zeta = 0; \qquad \text{at infinity (i.e. } \xi = 0) \tag{13}$$

$$\psi^* = 0, \qquad \zeta = 0; \qquad \text{at } \eta = 0,\ \eta = 1 \quad \text{(symmetry axis)} \tag{14}$$

and, at the bubble surface,

$$\left.\begin{aligned} &\psi^* = 0 && \text{(zero normal velocity)} \\ &\zeta + 2\kappa^{(\xi\eta)}_{(n)} u_s = 0 && \text{(zero tang. stress)} \\ &-\frac{3}{4}C_D x - p_d + \tau_{nn} + \frac{4}{We}\left(\kappa^{(\xi\eta)}_{(n)} + \kappa^{(\xi\phi)}_{(n)}\right) = 0 && \text{(normal stress balance)} \end{aligned}\right\} \quad \text{at } \xi = 1 \tag{15, 16, 17}$$

The first term in (16) is the hydrostatic pressure; C_D is the drag coefficient; p_d is the dynamic pressure

$$p_d = -u_s^2 - \frac{4}{Re}\int \frac{1}{\sigma h_\xi}\frac{\partial}{\partial\xi}(\sigma\zeta)h_\eta d\eta \tag{18}$$

u_s is the surface velocity; τ_{nn} is the normal component of viscous stress at the surface, $We = \frac{d\rho v_\infty^2}{\gamma}$; γ is the surface tension, and $\kappa^{(\xi\eta)}_{(n)}$ and $\kappa^{(\xi\phi)}_{(n)}$ are normal curvatures in two perpendicular directions.

Numerical scheme

In order to solve Eqs. (7) and (8) of the preceding section, together with Eqs. (5a) and (5b) for the mapping functions $x(\xi,\eta)$ and $\sigma(\xi,\eta)$, we used a uniform 41x41 grid in the domain, $0 \le \xi,\eta \le 1$. The computations were carried out using single precision arithmetic on a VAX-11 computing system, which has a round-off error of $O(10^{-6})$. Thus, with an $O(h^2)$ finite-difference scheme, this mesh size represents the practical limits of resolution in order that truncation error be comparable to this round-off error divided by h^2 (when computing second derivatives).

The numerical scheme itself must be fast, highly stable and applicable to elliptic equations of quite general form. In the work reported here, we adopt the ADI scheme of Peaceman and Rachford and treat all equations of the problem (i.e. the equations of motion for ζ and ψ, and the two mapping equations for x and σ) as "quasi-time-dependent", by writing them in the standard form

$$\frac{\partial w}{\partial t} = q_1 \frac{\partial^2 w}{\partial \xi^2} + q_2 \frac{\partial^2 w}{\partial \eta^2} + q_3 \frac{\partial w}{\partial \xi} + q_4 \frac{\partial w}{\partial \eta} + q_5 w + q_6 \tag{19}$$

with $\partial/\partial t$ representing a "fictitious" (or artificial) time derivative as required by ADI. An optimal value of the iteration parameter (i.e. time step) was determined[14] to be O(h).

Boundary conditions for Eqs. (3), (5) and (6) are straightforward [see Eqs. (13)-(16) plus Ref. 6], with the exception fo conditions at the bubble surface. Here, the necessary boundary values of vorticity are calculated indirectly from the boundary condition (16) on tangential stress using a natural extension of the method for a solid boundary suggested by Dorodnitsyn and Meller[15] and Israeli[16] and utilized previously for a spherical drop.[17] At each new iteration, say n, the new value of the boundary vorticity ζ^n is determined from its previous value and the previous value of the tangential stress, as

$$\zeta^n = \zeta^{n-1} + \beta\left(-2\kappa_{(n)}^{(\xi\eta)} u_s^{n-1} - \zeta^{n-1}\right) \tag{20}$$

where the optimal β was found (by trial and error) to be approximately 0.2. When the solution has converged, of course, the tangential stress will be zero. Boundary conditions for $x(\xi,\eta)$ and $\sigma(\xi,\eta)$ at $\xi = 1$ must also be discussed briefly. Both x and σ cannot be specified directly at $\xi = 1$ if the condition $g_{12} = 0$ is satisfied (i.e. the coordinates are to be orthogonal) as the problems for x and σ are then overdetermined. We would, on the other hand, like to approach the final solution for bubble shape iteratively starting from some initial guess. This involves incrementing the bubble boundary to create a new shape at each iteration, based upon the normal stress imbalance at the interface at the preceding iteration. However, in view of the restriction on simultaneous specification of x and σ, the necessary small displacement of the bubble boundary must be carried out indirectly rather than specifying increments in $x(1,\eta)$ and $\sigma(1,\eta)$ directly. This is accomplished by changing the mapping itself (rather than the position of the bubble surface) via incremental changes in the scale factor h_ξ of the mapping, i.e.

$$h_\xi^{(n+1)}\Big|_{\xi=1} = h_\xi^{(n)}\Big|_{\xi=1} \left(\frac{4\pi}{(\mathrm{vol})^n}\right)^{1/3} + \beta_G \cdot \Delta^n \tag{21}$$

where Δ^n is the normal stress imbalance at iteration n,

$$\Delta = -\frac{3}{4} C_D x - p_d + \tau_{nn} + \frac{4}{We}\left(\kappa_{(n)}^{(\xi\eta)} + \kappa_{(n)}^{(\xi\phi)}\right). \tag{22}$$

The incremented $h_\xi\big|_{\xi=1}$ is then used to generate "equivalent" boundary conditions for

$$\frac{\partial x}{\partial \xi}\bigg|_{\xi=1} \quad \text{and} \quad \frac{\partial \sigma}{\partial \xi}\bigg|_{\xi=1} \tag{23}$$

The normal stress difference, Δ, has to be normalized before it is used in (21) for changing the bubble shape because of the indeterminacy due to incompressibility (Δ contains an integration constant); this indeterminacy is removed by requiring that the volume of the bubble remain constant.

The overall solution algorithm may thus be schematically represented as follows:

(1) Start with an initial guess of the shape. Here we choose a spherical shape, i.e. a circle in a plane through the axis of symmetry. Hence, with $f(\xi,\eta) = \pi\xi$ as indicated earlier, the mapping is initially $x = \xi\cos\pi\eta$ and $y = \xi\sin\pi\eta$, corresponding to polar coordinates in the plane through the axis of symmetry.

(2) For the given bubble shape and coordinate mapping, compute a new approximation for the dynamic fields (ψ and ζ) by advancing the solution of the Navier-Stokes equations one iteration (i.e. one ADI time step).

(3) Calculate the normal stress terms at the bubble surface, and if the condition (17) is not satisfied, increment the bubble shape by a small amount by incrementing $h_\xi(1,\eta)$ using Eq. (21), and obtaining corresponding boundary conditions for $\partial x/\partial\xi\big|_{\xi=1}$ and $\partial y/\partial\xi\big|_{\xi=1}$.

(4) Calculate a new orthogonal mapping fitting the new bubble shape by solving Eqs. (5a,b) with appropriate boundary conditions (in practice we do only one ADI iteration on the mapping equations).

(5) Repeat this process starting with step (2) until convergence is achieved.

Results

We consider two cases here of streaming flow past a bubble.

Case A: Re = 2.47, We = 4.00
Case B: Re = 100., We = 2.00

The final bubble shape is depicted for Case A in Fig. 1, where we show a portion of the final coordinate mesh and the upper half of the bubble boundary in the plane through the axis of symmetry. The flow is from left to right. The corresponding streamlines and lines of constant vorticity are shown in Figs. 2 and 3. It may be noted that the bubble shape is in qualitative agreement with available experimental results.[18] Indeed, the drag coefficient calculated here is 9.17, whereas the measured value at the same Reynolds number but somewhat larger We was 9.37. It may be noted that the drag coefficient was found experimentally[18] to be insensitive to We for large We. The streamlines and lines of constant vorticity for Case B are shown in Figs. 4 and 5, from which the bubble shape can also be discerned. Again, the flow is from left to right. It is thus evident that the bubble is actually flattened to a greater degree in the front and is more rounded at the rear. Shapes of this general type have been previously observed experimentally for similar values of Re and We,[19] although a shape which is rounded in the front and flattened at the rear, which will occur for larger Reynolds number or larger Weber number, i.e. smaller surface tension, is much more common. Each example required about an hour of CPU time on a VAX-11 computer, starting from the irrotational flow pas a sphere as an initial guess in both cases. The cost is thus on the order of $10.

Acknowledgments

This work was supported by a grant from the fluid mechanics program of the National Science Foundation.

References

1. Taylor, T. D. and Acrivos, A., "On the Deformation and Drag of a Falling Viscous Drop at Low Reynolds Number", J. Fluid Mech. 18, 466-476 (1964).
2. Cox, R. G., "The Deformation of a Drop in a General Time-Dependent Fluid Flow", J. Fluid Mech. 37, 601-623 (1969).
3. Youngren, G. K. and Acrivos, A., "On the Shape of a Gas Bubble in a Viscous Extensional Flow", J. Fluid Mech. 76, 433-442 (1976).
4. Miksis, M., Vanden-Broeck, J.-M. and Keller, J. B., "Axisymmetric Bubble or Drop in a Uniform Flow", J. Fluid Mech. 108, 89-100 (1981).
5. Rallison, J. M., "A Numerical Study of the Deformation and Burst of a Viscous Drop in General Shear Flows", J. Fluid Mech. 109, 465-482 (1981).
6. Ryskin, G. and Leal, L. G., "Orthogonal Mapping", submited to J. Comp. Phys.
7. Thames, F. C., Thompson, J. F., Mastin, C. W. and Walker, R. L., "Numerical Solutions for Viscous and Potential Flow about Arbitrary Two-Dimensional Bodies Using Body-Fitted Coordinate Systems", J. Comp. Phys. 24, 245-273 (1977).
8. Fornberg, B., "A Numerical Method for Conformal Mapping", SIAM J. Sci. Stat. Comput. 1, 386-400 (1980).
9. Starius, G., "Constructing Orthogonal Curvilinear Meshes by Solving Initial Value Problems", Numer. Math. 28, 25-48 (1977).
10. Davies, C.W., "An Initial Value Approach to the Production of Discrete Orthogonal Coordinates", J. Comp. Phys. 39, 164-173 (1981).
11. Pope, S. B., "The Calculation of Turbulent Recirculating Flows in General Orthogonal Coordinates", J. Comp. Phys. 26, 197-217 (1978).
12. Hung, T.-K. and Brown, T. D., "An Implicit Finite-Difference Method for Solving the Navier-Stokes Equation Using Orthogonal Curvilinear Coordinates", J. Comp. Phys. 23, 343-363 (1977).
13. Mobley, C. D. and Stewart, R. J., "On the Numerical Generation of Boundary-Fitted Orthogonal Curvilinear Coordinate Systems", J. Comp. Phys. 34, 124-135 (1980).
14. Ames, W. F., "Numerical Methods for Partial Differential Equations", Barnes and Noble, New York, 1969.
15. Dorodnitsin, A. A. and Meller, N. A., "Approaches to the Solution of Stationary Navier-Stokes Equations", U.S.S.R. Comput. Math. & Math. Phys. 8(2), 205-217 (1968).
16. Israeli, M., "A Fast Implicit Numerical Method for Time Dependent Viscous Flows", Stud. Appl. Math. 49, 327-349 (1970).
17. Rivkind, V. Ya. and Ryskin, G., "Flow Structure in Motion of a Spherical Drop in a Fluid Medium of Intermediate Reynolds Numbers", Fluid Dyn. 11, 5-12 (1976).
18. Bhaga, D. and Weber, M. E., "Bubbles in Viscous Liquids: Shapes, Values and Velocities", J. Fluid Mech. 105, 61-85 (1981).
19. Clift, R. C., Grace, J. R. and Weber, M. E., "Bubbles, Drops and Particles", Academic Press, 1978.

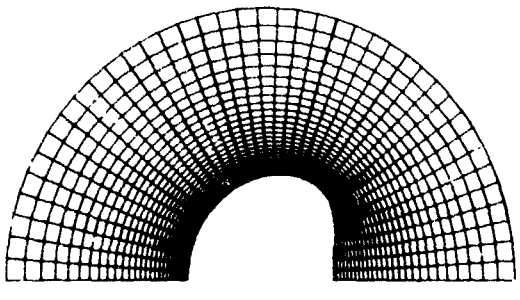

Figure 1. Coordinate mesh for Case A.

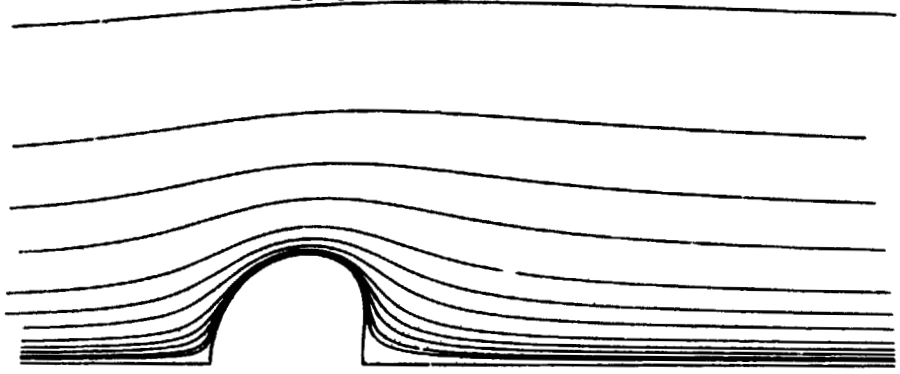

Figure 2. Streamlines for Case A.

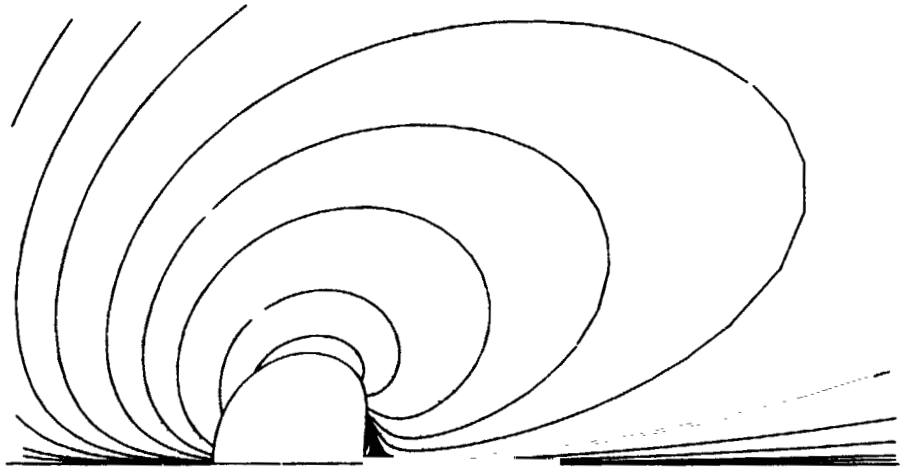

Figure 3. Lines of constant vorticity for Case A.

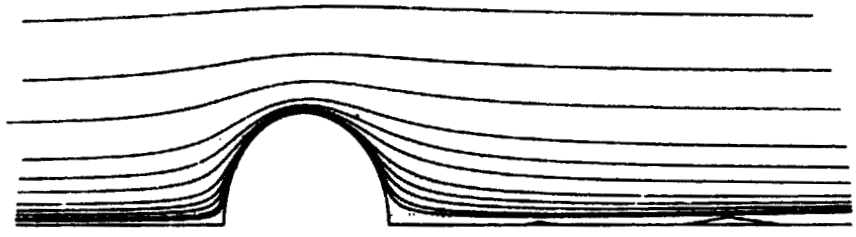

Figure 4. Streamlines for Case B.

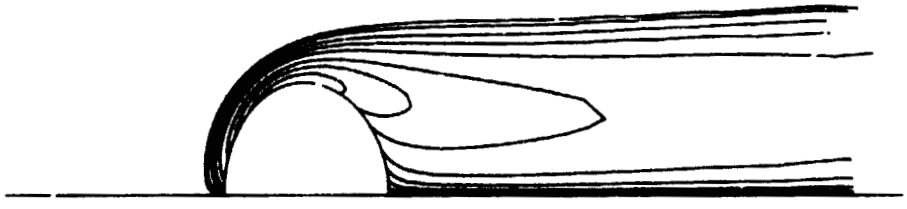

Figure 5. Lines of constant vorticity for Case B.